Vision Research 111 (2015) 43–54

Contents lists available at ScienceDirect

Vision Research

journal homepage: www.elsevier.com/locate/visres

Two mechanisms that determine the Barber-Pole Illusion

Peng Sun [a,b,*], Charles Chubb [a], George Sperling [a]

[a] Department of Cognitive Sciences, University of California Irvine, Irvine, CA 92617, United States
[b] Department of Psychology, New York University, New York, NY 10003, United States

ARTICLE INFO

Article history:
Received 17 December 2014
Received in revised form 5 April 2015
Available online 11 April 2015

Keywords:
Motion perception
Barber-Pole-Illusion
Shape–motion-interaction
2D motion

ABSTRACT

In the Barber-Pole Illusion (BPI), a diagonally moving grating is perceived as moving vertically because of the narrow, vertical, rectangular shape of the aperture window through which it is viewed. This strong shape–motion interaction persists through a wide range of parametric variations in the shape of the window, the spatial and temporal frequencies of the moving grating, the contrast of the moving grating, complex variations in the composition of the grating and window shape, and the duration of viewing. It is widely believed that end-stop-feature (third-order) motion computations determine the BPI, and that Fourier motion-energy (first-order) computations determine failures of the BPI. Here we show that the BPI is more complex: (1) In a wide variety of conditions, weak-feature stimuli (extremely fast, low contrast gratings, 21.5 Hz, 4% contrast) that stimulate only the Fourier (first-order) motion system actually produce a slightly better BPI illusion than classical strong-feature gratings (2.75 Hz, 32% contrast). (2) Reverse-phi barber-pole stimuli are seen exclusively in the feature (third-order) BPI direction when presented at 2.75 Hz and exclusively in the opposite (Fourier, first-order) BPI direction at 21.5 Hz, indicating that both the first- and the third-order systems can produce the BPI. (3) The BPI in barber poles with scalloped aperture boundaries is much weaker than in normal straight-edge barber poles for 2.75 Hz stimuli but not in 21.5 Hz stimuli. Conclusions: Both first-order and third-order stimuli produce strong BPIs. In some stimuli, local Fourier motion-energy (first-order) produces the BPI via a subsequent motion-path-integration computation (Journal of Vision (2014) 14, 1–27); in other stimuli, the BPI is determined by various feature (third-order) motion inputs; in most stimuli, the BPI involves combinations of both. High temporal frequency, low-contrast stimuli favor the first-order motion-path-integration computation; low temporal frequency, high-contrast stimuli favor third-order motion computations.

1. Introduction

1.1. The Barber-Pole Illusion

Three classic theories of motion perception (Adelson & Bergen, 1985; Van Santen & Sperling, 1984, 1985; Watson & Ahumada, 1985) assert that, at an early stage of visual processing, motion signals are extracted by neural mechanisms that essentially compute the Fourier energy of the spatiotemporal luminance patterns within their local neighborhoods. For a translating sinusoidal grating, such Fourier-energy based mechanisms signify a direction of motion that is perpendicular to the orientation of the grating. However, in a Barber-Pole Illusion (BPI) such as the one shown in Fig. 1, a diagonally moving grating appears to move vertically when viewed through a vertically-orientated rectangular window (Wallach, 1935).

The BPI suggests that the perceived direction of a motion stimulus is determined not just by local motion energy but also by the shape of the aperture within which the motion signal is visible. To account for such form-motion interaction, requires further elaboration of the existing motion theories that are concerned only with local Fourier energy. Here we revisit previous demonstrations of shape–motion interactions in barber-pole stimuli and present new demonstrations that better define the visual computations involved in producing the BPI.

1.1.1. The Fourier components in barber-pole stimuli

The sensitivity of the lower-level, first-order motion system is well-described by its responses to the Fourier components of the motion stimulus (Chubb & Sperling, 1988; Emerson, Bergen, & Adelson, 1992; Lu & Sperling, 1995b, 1999, 2001; Van Santen & Sperling, 1984, 1985). The barber-pole stimulus is the product $W(x,y)G(x,y,t)$ of a spatial aperture $W(x,y)$ times a drifting

* Corresponding author at: Department of Psychology, New York University, New York, NY 10003, United States.
E-mail address: peng.sun@nyu.edu (P. Sun).

http://dx.doi.org/10.1016/j.visres.2015.04.002
0042-6989/

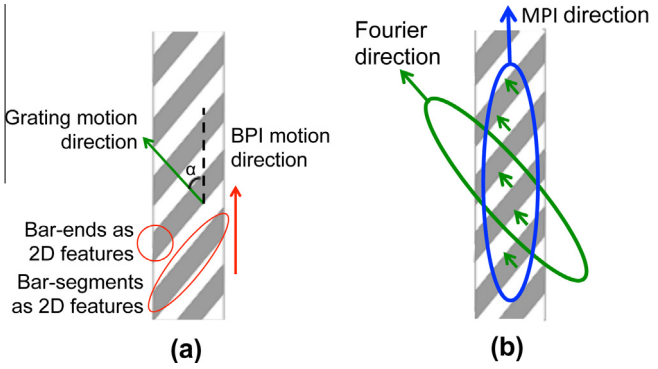

Fig. 1. Illustration of a classical barber-pole display. (a) A classic barber-pole. The physical direction α of grating motion is the direction of the dominant Fourier component(s) of the moving grating; this direction is perpendicular to the grating stripes. However, when viewed through a vertical aperture (e.g., an aperture with the 4:1 vertical:horizontal aspect ratio illustrated here), a grating consisting of diagonally translating bars appears to move vertically, the Barber-Pole Illusion (BPI). Indeed, the barber-pole display does contain unambiguous vertical motion signals carried by the vertical movement of 2D spatial features such as bar-segments and bar-ends. (b) Simplified illustration of the Motion-Path-Integration (MPI) theory (Sun, Chubb, & Sperling, 2014). Ovals in blue and green represent two of many different spatial paths along which local motion energy (short arrows) that has a component in the direction of the path is integrated. Only spatial (and not temporal) integration components of the MPI theory are illustrated here. (For interpretation of the references to color in this figure legend, the reader is referred to the web version of this article.)

sinusoidal grating $G(x, y, t)$. Therefore the Fourier transform of the barber-pole stimulus is simply the convolution of the spatial Fourier transform of W with spatiotemporal Fourier transform of G. The Fourier spectrum of a barber-pole stimulus such as Fig. 1 contains the Fourier components of the aperture $W(x, y)$ splattered symmetrically around each of the Fourier components of the grating $G(x, y, t)$. If the barber pole were simply a single pixel wide, then the barber-pole stimulus would consist of spots moving vertically, and the Fourier analysis would, of course, confirm this. What is not so obvious, however, is that as soon as the barber-pole aperture is wide enough to include just two pixels, the visually important Fourier components signify motion in the diagonal direction, i.e., perpendicular to the grating stripes (see Appendix A).

For practical purposes, the dominant Fourier component, or a pool of the responses of all the visible Fourier components of a barber-pole stimulus, always signifies the direction perpendicular to the orientation of the grating. This means that neurons in visual area V1 that respond to sinewave motion – and nearly all the motion-sensitive neurons do – will signal the diagonal direction, and not the BPI direction. Therefore, accounting for the BPI requires either different kinds of basic motion detectors, e.g., feature detectors or, as we show below, higher-level mechanisms that combine the outputs of the local Fourier motion detectors. The role of feature detectors in the BPI is well established, e.g., (Lorenceau, 2010). Here we present a further characterization of the feature detectors involved in the BPI, new evidence for a higher-order motion-path-integration mechanism, and a road map to show the conditions under which these mechanisms are active.

1.1.2. BPI: the unambiguous motion of 2D spatial features

1.1.2.1. Moving bars. A motion generated by a spatially 1D moving pattern (e.g. a drifting sinusoidal grating) is intrinsically ambiguous because the component of velocity in the spatially invariant pattern dimension cannot be detected. By contrast, the motion direction and speed (velocity) of a 2D moving feature (e.g. a spot, a corner, or a line end) moving in a 2D plane is absolutely unambiguous. A classic barber-pole stimulus contains 2D spatial features that move unambiguously parallel to the boundary of the aperture window. In the barber-pole stimulus illustrated in Fig. 1, all the bar segments inside the aperture move veridically upward along the vertical boundary of the aperture window. Therefore a theory based on a mechanism that tracks the movements of the bar segments could explain the BPI (e.g. Marshall, 1990).

1.1.2.2. Moving end-stops. An alternative explanation of the BPI attributes it to the computation of the bar-ends. This theory is known as the "end-stop" theory (see Lorenceau (2010) for a review). The "end-stop" theory is consistent with many factors known to affect the strength of the BPI. For example, when the relative angle α (see Fig. 1a) is made smaller so that the number of the bar terminators on the vertical boundary decreases, the BPI becomes weaker (Fisher & Zanker, 2001).

The BPI also is weaker when the boundary on the longer side of the aperture is made to appear in a different depth plane than the moving grating, due to various kinds of depth cues (Castet, Charton, & Dufour, 1999; Lidén & Mingolla, 1998; Shimojo, Silverman, & Nakayama, 1989). Bars and the off-plane aperture boundary form "extrinsic end-stops" that are not classified as genuine features, thus cannot generate a strong feature motion.

Less direct support comes from the similarity between the BPI's temporal dynamics and the temporal dynamics of the perceived motion direction of moving line segments. Moving line segments initially appear to move perpendicularly to the line segments' orientation, and the perceived motion direction shifts towards their actual motion direction as exposure duration increases (Lorenceau et al., 1993). Similarly, the perceived motion direction of a classic barber-pole display is initially perpendicular to the grating's orientation, and gradually shifts towards the BPI motion direction (Masson et al., 2000). This pattern of dynamics has been explained in terms of the slower processing time of the "end-stop" mechanism relative to the Fourier motion-energy computation (Pack et al., 2003).

However, some BPI results are inconsistent with the end-stop explanation. When the line grating within an elongated aperture window contains gaps so that interior line-ends also carry unambiguous diagonal motion signals, perceived motion is not in the diagonal motion direction of the interior line-ends. Instead, the complex pattern appears as dashed lines moving along the longer side of the aperture (Castet & Wuerger, 1997). Furthermore, when a plaid pattern (two superimposed gratings) moves inside an elongated aperture, the perceived motion direction of the plaid is biased in the aperture's orientation (Beutter, Mulligan, & Stone, 1996) even though the plaid is moving unambiguously in a different direction.

Recently, Sun, Chubb, and Sperling (2014) introduced a novel moving barber-pole display in which the apertures (the barber poles) and the gratings (the movements within the barber poles) move independently. Because of the movement of the aperture, the 2D motion of the spatial features in the moving-barber-pole stimulus is no longer in the aperture's elongated orientation. In a moving barber-pole display with vertical barber-poles, the movement of features such as bar segments and bar ends is consistent with a specific, rigid direction of diagonal motion. Nevertheless, in peripheral viewing, stimuli of this sort evoke purely vertical motion for a wide range, but not all, of tested conditions. Perceiving vertical motion while all barber-pole features move diagonally implies that, at least in the moving-barber-pole stimulus, other factors than feature motion determine the BPI.

1.1.3. The motion streak theory of the BPI

Badcock, McKendrick, and Ma-Wyatt (2003) found that the BPI was weakened substantially when the barber-pole aperture's

boundary contained variations in local direction that deviated from the predominant direction of the aperture boundary. To account for these results, these investigators suggested that the aperture boundary acted like the motion streak to produce the BPI. According to this theory, an aperture boundary containing irregular, local variations in direction produces a weaker BPI than a smooth aperture boundary because the non-smooth boundary is not consistent with spatial patterns produced by motion streaks.

Implicit in the motion streak theory is a mechanism that combines motion information with static pattern information. The motion streak theory can qualitatively explain some BPI phenomena that are inconsistent with the "end-stop" theory but it cannot, for example, explain the perceived vertical motion in the moving BPI in which spatial vertical patterns are rendered less visible.

1.1.4. The motion-path-integration (MPI) theory of the Barber Pole Illusion (BPI)

To explain a wide range of BPI phenomena, Sun, Chubb, and Sperling (2014) proposed a theory of the BPI based on integrating local motion energy for a limited time period along each of various spatial paths (Fig. 1b). The path with the greatest path-motion energy is selected as the predicted motion direction. For classical and for moving barber-pole displays, the path with the greatest motion energy is close to the aperture's elongated orientation, i.e., the BPI. This can be easily seen in 1b. Integrating along the red path brings in continuous local motion energy whereas the green path is interrupted by regions containing zero motion energy on both sides of the barber-pole aperture (See Fig. 15 in Sun, Chubb, and Sperling (2014) for a more detailed explanation).

On the other hand, the motion-path-integration (MPI) theory makes similar predications for barber-pole displays with smooth and with irregular aperture boundaries. This is because integrating local motion energy is more sensitive to the global shape of the integral path and less sensitive to the local variations in the integral path's boundary. Therefore the MPI theory cannot explain the effect of the aperture boundary on the strength of the BPI reported in Badcock, McKendrick, and Ma-Wyatt (2003).

1.2. Multi-system motion theory

1.2.1. Differentiable characteristics of motion systems

Lu and Sperling (1995b, 2001) proposed a three-system theory to account for different classes of motion perceptual experiences. The first-order system computes local Fourier energy from moving luminance modulations. Although first-order motion often is called luminance motion, the operative variable for first-order motion is the Weber contrast $C(x,y,t)$ of the input stimulus at each point (x,y) in space at each time t. That is,

$$C(x,y,t) = \frac{L(x,y,t) - \mu_L(x,y,t)}{\mu_L(x,y,t)} \quad (1)$$

where $L(x,y,t)$ is the luminance of the input stimulus at point (x,y) at time t, and $\mu_L(x,y,t)$ is the average luminance of the input in local neighborhood of (x,y) immediately prior to time t. It is critical for the first-order motion computation that $C(x,y,t)$ can be either negative or positive, whereas luminance, by definition, is always nonnegative.

The second-order system extracts motion from spatiotemporal variations in *pattern contrast*, i.e., from the local variance of $C(x,y,t)$.

The third-order system extracts motion from spatiotemporal variations in a *salience map* of the visual input. The salience $S(x,y,t)$ at a point (x,y) in visual space at a given time t is hypothesized to be a scalar quantity that depends on the same factors that promote some regions in a scene to be perceived as "figure" (high salience) and demote others to be perceived as ground (low salience).[1] When we here refer to "feature motion" or to "tracking", it is to be understood that it refers to a motion computation by the third-order motion system.

The first- and third-order systems are the ones activated by our experimental stimuli. The relevant properties of these motion extraction systems are:

- The first-order system has excellent spatial acuity and can process luminance modulations over a broad range of temporal frequencies. Its sensitivity declines significantly only above about 16 Hz.
- The third-order system is more versatile in terms of what stimuli it can process. Insofar as a feature (which may be defined by luminance contrast, color, binocular disparity, etc.) is significantly more salient than its surround, the third-order system can compute the salient feature's motion. The versatility of the third-order motion-perception system is achieved at a cost in spatial and temporal resolution. Third-order motion sensitivity declines quickly above 3–4 Hz (Lu & Sperling, 2001, 1995b). Also, compared to the first-order system, the relative power of the third-order system declines more rapidly as eccentricity increases, typically because the third-order system's spatial resolution limit is exceeded.

1.2.2. The significance of the multi-system motion theory

Most experimentally-studied stimuli stimulate more than just one motion system. The failure to appreciate this fact has led to a great deal of confusion in the field of motion perception. For example, the question of how a plaid motion (two superimposed moving sinusoidal gratings) is computed by the motion system has been debated extensively over the past few decades. One of the competing theories argues that the perceived plaid motion results from summing each of the two component motion vectors. Another theory argues that the plaid motion processing mechanism tracks the motion of the intersections of the two sinusoidal gratings. Empirical support has been garnered for each theory; however, a careful review of the available evidence reveals that the two theories operate most effectively over different parametric ranges of plaids. The participants of Sperling and Liu (2009) produced responses consistent with one or the other theory depending on the temporal frequency and the contrast of the plaid stimulus. In particular, the direction of perceived motion followed the path of the intersections for plaids of high contrast and low temporal frequency, a condition favored by the third-order system. On the other hand, the direction of perceived motion was given by a sum (weighted by relative amplitudes) of the plaid's two component motion vectors for plaids of low contrast and high temporal frequency, a condition favored by the first-order system. When stimulus contrast and the temporal frequency fell in an intermediate range, perceived plaid motion was given by an additive mixture of both computations. The above example illustrates that the first- and third-order motion perception systems operate concurrently to extract motion from the visual plaids, and it illustrates

[1] The third-order system is referred to as a "feature tracking" system, which reflects an unfortunate confusion. To track a moving object requires a prior motion computation. Otherwise, whenever an object appeared in a new location, that location would first need to be discovered by a search process to enable tracking. Another problem with the concept of feature tracking as a motion-perception mechanism is evident in certain alternating feature displays in which odd- and even-number frames are composed of different features so that tracking any single feature leads to completely ambiguous motion Lu and Sperling (1995a). To perceive motion requires combining feature salience in both even and odd frames. Although an observer may track a feature that occurs in the odd frames, its perceived direction is determined by features in the even frames that typically are unnoticed.

the conditions that favor each system. We propose to apply the same principles to the study of barber-pole stimuli.

1.3. Aim of the study

How do first-order and third-order motion perception processes affect the BPI, and how does this explain the effect of the various stimulus manipulations on the BPI? Experiment 1 is a baseline control experiment under conditions favorable for both first- and third-order motion perception systems to measure the perceived motion direction of barber-pole stimuli as a joint function of the aspect ratio of the barber-pole aperture and the angle of the moving grating. In Experiments 2, 3 and 4, the relative strengths of the contributions of the first- and of the third-order motion-perception systems to the barber-pole stimulus are manipulated. In Experiment 2, stimulus temporal frequency and contrast are chosen to maximally favor either the first- or the third-order motion system in a variety of classical barber-pole stimuli. In Experiment 3, a reverse-phi barber-pole stimulus is perceived in opposite directions depending on temporal frequency of the moving grating. Experiment 4 shows that scalloped edges of the barber-pole aperture affect perceived direction of motion differently depending on whether the moving grating's temporal frequency and contrast favor first- or third-order motion perception.

2. General method, all experiments

2.1. Apparatus

The experiments were controlled by a Macintosh Intel computer running Matlab with the Psychtoolbox package (Brainard, 1997). Stimuli were displayed on a 15-inch Mitsubishi Diamand Pro 710S VGA monitor with 1024 by 768 resolution running at 85 Hz refresh rate. The stimuli were created from a gamut of 256 equally-spaced gray levels. The mean luminance of all the stimuli and of the background was 52.1 cd/m^2.

2.2. Subjects

Three participants (S1, S2 and S3) took part in Experiments 1, 2 and 3; an additional participant was recruited for Experiment 4. Although all had previously participated in psychophysical experiments, none had participated in experiments involving motion perception. All were naive to the purpose of the study. All methods used were approved by the UC Irvine institutional review board, and in accordance with The Code of Ethics of the World Medical Association (Declaration of Helsinki). All participants provided signed informed consent forms.

2.3. Procedure

In all experiments, stimuli were viewed binocularly at a distance of 60 cm. A clock face circumscribed the center of the screen (Fig. 2) throughout the session. Participants were instructed to maintain fixation at its center throughout stimulus presentation. After fixating the center of the display region, the participant initiated a trial by pressing a button; 400 ms later, a randomly oriented barber-pole stimulus appeared for 800 ms in the middle of the display region. The relatively long exposure duration of 800 ms was chosen to maximally advantage third-order (feature) motion relative to first-order motion (e.g., Lorenceau et al. (1993) and Sperling & Liu (2009)) and to enable comparison with studies by Badcock, McKendrick, and Ma-Wyatt (2003) which are here replicated in part. Following stimulus exposure, the participant clicked on the clock face with a mouse-controlled pointer to indicate the dominant direction of motion evoked by the stimulus. Before a formal experiment, participants conducted 50 practice trials.

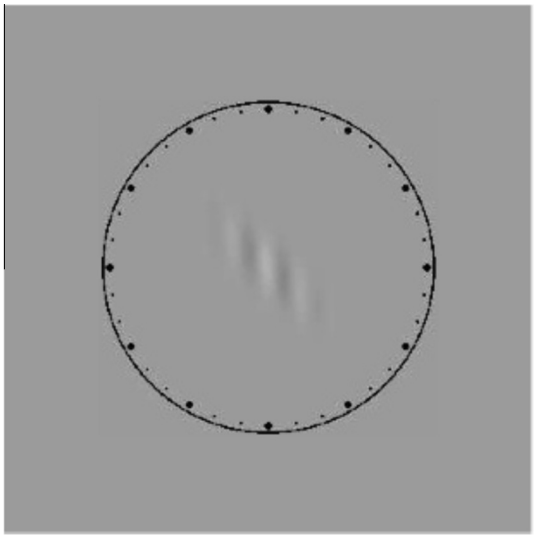

Fig. 2. The clock face used to record the perceived motion direction (PMD), and a sample stimulus. Subjects were instructed to fixate the center of the clock circle throughout the stimulus presentation. Following the 800 ms stimulus display, participants indicated their PMD by clicking on the corresponding position on the clock face using a mouse-controlled pointer. The clock face remained on the screen for the entire session.

3. Experiment 1: Barber-Pole Illusion (BPI) as a function of aperture aspect ratio and grating angle

The strength of the Barber-Pole Illusion (BPI) depends on the aspect ratio (height/width) of the aperture window and the relative angle α formed between the aperture's major axis and the direction of grating motion. The first experiment confirms this dependency to establish baseline performance.

3.1. Stimuli

A drifting sinusoidal grating was shown within an elliptical aperture window (Fig. 3). The grating had a spatial frequency of 1.2 c/d and translated at 5 Hz. These spatial and temporal frequencies are well perceived by both the first- and the third-order motion systems (Lu & Sperling, 1995b, 2001). The amplitude of the moving grating was modulated by a static elliptical Gaussian aperture. The aspect ratio of the ellipse was varied while keeping the visible area of the stimulus constant by fixing the product of the lengths of ellipse's axes. In each stimulus, the maximum contrast was 20%. For a circular Gaussian aperture (i.e., when the aspect ratio equalled 1), the area within which the contrast was above 0.2% (i.e., 1% of maximum contrast) had a radius of 1.73°.

Fig. 3 shows the six grating-to-aperture angles α ($0°, 30°, -45°, 60°, -75°, 90°$) as defined in Fig. 1 and four aspect ratios (1:1, 1.5:1, 3:1, 5:1) that were tested. For all 24 combinations of α and aspect ratio, 20 repetitions were generated, in each of which the entire barber-pole display appeared at a random orientation angle θ. The orientation angles were jittered around 20 evenly spaced angles that spanned the entire circle. That is, for p_k a random permutation of $k = 1, 2, \cdots, 20$ and ρ a random angle [−9,9], the 20 stimuli used in the repetitions of a given condition had orientations $\theta_k = \rho + p_k\pi/10$. In total, a full session had 480 trials. The entire experiment lasted about 1 h including breaks every 100 trials.

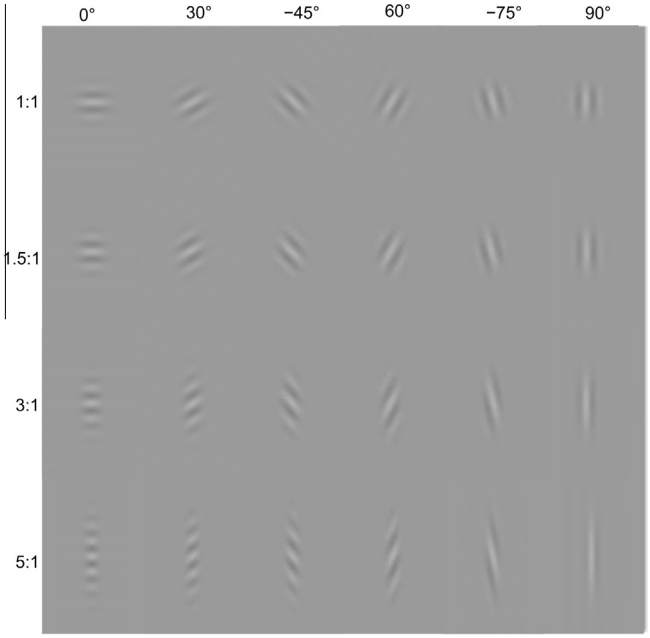

Fig. 3. Snapshots of the four aperture aspect ratios and six directions of grating movement of the barber-pole stimuli used in Experiment 1. From top to bottom, rows illustrate stimuli whose apertures have aspect ratios 1:1, 1.5:1, 3:1, and 5:1. The visible area of the stimulus is kept constant across different aspect ratios by fixing the product of the two axis-lengths. From left to right, columns illustrate stimuli with grating-to-aperture angles $\alpha = 0^\circ, 30^\circ, -45^\circ, 60^\circ, -75^\circ, 90^\circ$. Although all barber-pole displays are shown here in a vertical orientation, in the experiment, displays were presented in random orientations. Stimuli for $+\alpha$ and $-\alpha$ are mirror images of each other; we assume throughout that they produce equal PMDs. Each stimulus in Experiment 1 had maximum grating contrast equal to 20%.

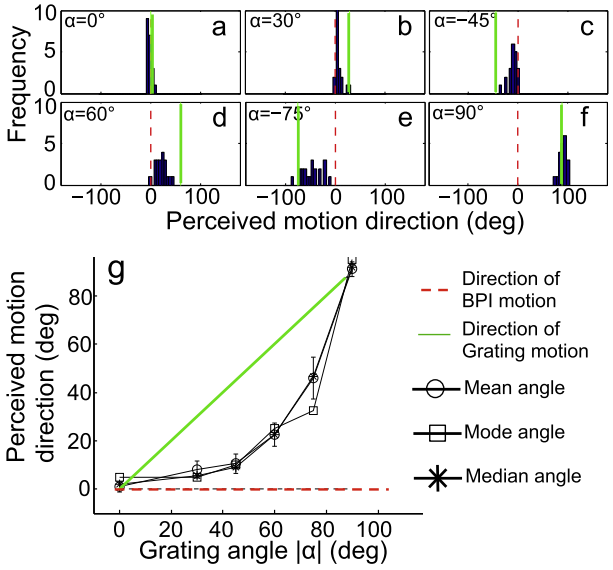

Fig. 4. Experiment 1: perceived motion direction for barber-poles gratings of six different angles. (a–f) Histograms of S1's perceived motion directions (PMDs) in a 5:1 barber-pole configuration for 6 different angles α of the moving grating. The solid green line indicates α, the direction of grating motion relative to the orientation of the barber pole's major axis (indicated by the dashed red line). (g) The mean (circles), median (squares) and mode (asterisks) of the subject's PMDs are plotted against $|\alpha|$. Only error bars for the mean are shown which represent 95% confidence intervals. Note that for the two $-\alpha$ angles, the signs of PMDs are flipped. (For interpretation of the references to color in this figure legend, the reader is referred to the web version of this article.)

3.2. Results and discussion

The data showed no measurable effects of absolute orientation θ of the grating aperture so the results are pooled over θ. In all plots, 0 gives the direction of motion parallel to the grating aperture (the BPI direction). The perceived motion directions (PMDs) are plotted as a function of $|\alpha|$, the angle of the grating relative to the long axis of the barber-pole aperture.

Fig. 4a–f show the histograms of participant S1's PMDs for barber-pole stimuli with aperture aspect ratio 5:1 across six grating angles α. Note that the histograms are strongly skewed towards the BPI direction for grating angles α up to about $\alpha = -45^\circ$. For an extreme angle, $\alpha = -75^\circ$, the histogram of S1's PMDs is more spread out. For $\alpha = 90^\circ$, only the direction perpendicular to the BPI is possible. The mean, median and mode of the PMDs are plotted against $|\alpha|$ in Fig. 4g. Since the three measurements are very similar, only the mean of PMDs is shown in all future figures.

Fig. 5 shows the full set of PMDs for 3 participants × 4 aperture aspect ratios × 6 angles αof grating motion. When the aperture aspect ratio is 1:1, the observed PMDs coincide precisely with direction of physical movement for all directions α of grating movement (the diagonal solid lines in Figs. 4g and 5). As aspect ratio increases, PMDs deviate from the grating motion direction towards the BPI direction. The higher the aspect ratio, the stronger the BPI. The strength of BPI also depends on α, with smaller αs producing stronger BPI. These results are consistent with previous studies (e.g., Fisher & Zanker, 2001) that showed similar dependencies of the BPI on the angle of the grating and the aspect ratio of the aperture.

4. Experiment 2: using temporal frequency and stimulus contrast to select either the first- or the third-order motion system

The third-order motion system can extract the motion of the spatial features in barber-pole stimuli provided they are of sufficient contrast and in a location of the visual field that has sufficient spatial and temporal resolution (Lu & Sperling, 1995a, 1999, 2001). On the other hand, the third-order motion system typically fails to process: (1) the motion direction of low-contrast spatial features such as low-contrast bar terminators in the barber-pole display (Lorenceau et al., 1993; Weiss, Simoncelli, & Adelson, 2002), (2) the motion direction of features moving at high temporal frequencies (Sperling & Liu, 2009), (3) the motion direction of peripherally viewed features (Lorenceau & Shiffrar, 1992; Lu & Sperling, 1999; Yo & Wilson, 1992). When those aspects of the barber-pole stimulus that stimulate the third-order system are weakened or entirely removed, it leaves only the first-order system to process the stimulus. (The second-order motion system, which deals primarily with variations in texture energy, is not relevant for barber-pole stimuli.) In barber-pole stimuli, the first-order system, as it is usually understood, would produce the perception of diagonal motion – the motion direction of the moving grating – not the BPI.

In complex dynamic visual patterns (not barber-poles), when higher-order motion was weakened or eliminated, and only the first-order motion system was stimulated, the perceived motion was in the Fourier direction. For example, by removing "end-stops" and thereby silencing the third-order system, Rubin and Hochstein (1993) found that two non-parallel, non-intersecting lines evoked a global motion percept whose direction was judged to be between the directions perpendicular to the two lines. For a single moving line, the perpendicular direction is the direction of the Fourier component motion of the line. Rubin and Hochstein (1993)'s result

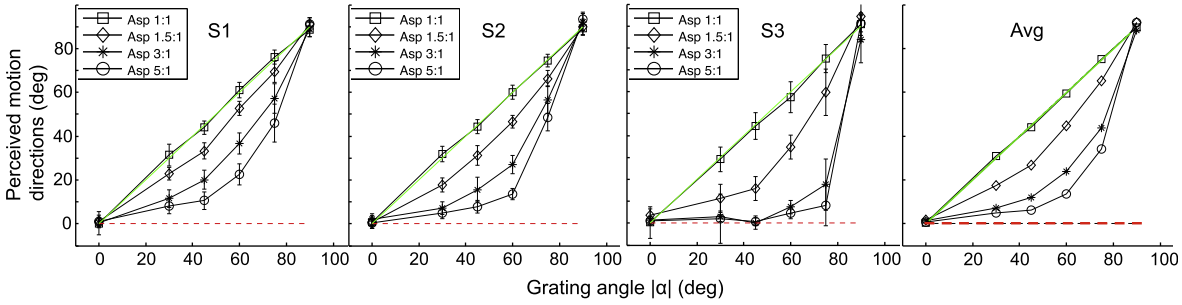

Fig. 5. Results of Experiment 1 for all three participants. Mean perceived motion direction (PMD) for 3 participants *times* four aperture aspect ratios *times* 6 grating angles α. Lines connect PMDs obtained with the same aspect ratio; symbols represent the different aspect ratios. Other notation as in Fig. 4.

shows that the first-order system, when processing Fourier component motions in two different directions, constructs a weighted summation of the two component motion vectors. Similarly, by weakening the third-order motion system so that the first-order system became dominant, Sperling and Liu (2009) demonstrated that a plaid stimulus appeared to move, not in the direction of feature motion, but in between the directions orthogonal to the two component gratings. In these stimuli, the first-order system responded to the Fourier component motion vectors in the stimulus by algebraically adding them. These results therefore suggest that whenever the third-order motion system is silenced, and only the first-order motion system is available to compute the motion of a barber-pole stimulus, only diagonal motion (the direction of "motion energy") should be perceived, absolutely no BPI (See Appendix A).

Experiment 2 attempts to silence the third-order motion system in order to determine the extent to which the BPI survives when only the first-order motion system is operative. And conversely, to minimize the first-order system's contribution and thereby to demonstrate the BPI with primarily feature (third-order) motion. Obviously, the BPI is expected to thrive in pure third-order motion stimuli. Insofar as the BPI survives even when there is only first-order (Fourier) motion input, one must conclude that the BPI results from a more complex computation that is neither third-order motion nor in the direction of Fourier (first-order) motion-energy.

4.1. Stimuli

Experiment 2 investigates barber-pole stimuli in which a diagonally moving sinewave grating is apertured by an elliptically shaped aperture with steep edges. That is, the Michelson contrast of the moving grating was constant within the aperture and zero elsewhere. The steep barber-pole edge is designed to enhance the end-stop features. Two types of barber-pole stimuli were produced, both of which used gratings with a spatial frequency of 1.2 c/deg: Strong-feature stimuli were designed to strongly stimulate the third-order motion system, whereas weak-feature stimuli were designed to be invisible to the third-order motion system but still highly visible to the first-order motion system. In the strong-feature condition, a sinusoidal grating with 32% contrast moved at a temporal frequency of 2.75 Hz. In the weak feature condition, a sinusoidal grating with a 4% contrast moved at a temporal frequency of 21.5 Hz.

Most observers cannot detect third-order motion at frequencies above 10 Hz (Lu & Sperling, 1995b, 2001). For an occasional observer, it is necessary to increase temporal frequency to 15 Hz in order to reduce the output of the third-order motion system below detection threshold (Sperling & Liu, 2009). The combination of a contrast of 4% (which is barely visible to the third-order system) and a 21.5 Hz temporal frequency (which is invisible to the third-order system even at maximum contrast) should guarantee total silence of the third-order system.

Three aspect ratios of the elliptical aperture (1.5:1, 3:1, 5:1), four relative angles of the moving grating ($-15^\circ, 30^\circ, -45^\circ, 60^\circ$), 30 different overall orientations of the display ($0 - 359^\circ$), 2 trials of each type, comprised a mixed list of 720 trials. The total area of the aperture was kept the same for all the different aperture aspect ratios. The same participants served as in Experiment 1. As in all the experiments herein, the participants indicated the perceived motion direction (PMD) by clicking on the clock face. The entire mixed-list test took about 1.5 h including breaks after every 100 trials.

4.2. Results and discussion

Fig. 6 shows the PMDs for the strong- and weak-feature conditions for each participant for each combination of aperture ratio and relative direction $|\alpha|$ of the moving grating, averaged over the various display orientations and reflections. In these hard-edged elliptical apertures, the strong Barber-Pole Illusion (PMDs concentrated within about $\pm 10^\circ$ in direction of the aperture's primary axis) is observed only for aspect ratios of 3:1 and 5:1, and then only for relative directions $|\alpha|$ for which $|\alpha| = 30^\circ$ and $|\alpha| = 45^\circ$. In apertures with an aspect ratio of 1:1.5, the Fourier direction of motion dominates. In the other conditions, the PMD is a compromise between the feature direction (third-order motion) and the Fourier direction (α, the first-order motion direction). The Fourier direction dominates more and more as the aperture aspect ratio decreases and as grating angle α increases.

However, what is most significant in the data of Fig. 6 is that the strong-feature and weak-feature conditions produce remarkably similar PMDs. In fact, the weak-feature conditions (which effectively eliminate third-order motion, i.e., eliminate "feature tracking") produce PMDS that are equal to or closer to the BPI than the strong feature conditions.[2] This is surprising because the stimuli of Experiment 2 had step-edge apertures that were intended to maximally emphasize end-stop features. That eliminating the possibility of feature tracking in the weak-feature stimuli actually strengthens the BPI (relative to the matched strong-feature stimuli) means that even in the strong-feature stimuli that maximally favor feature tracking, feature tracking probably is not the only cause of the BPI. The remarkable similarity of the PMDs in weak and strong feature stimuli strongly suggests that similar perceptual processes operate in both types of stimuli.

[2] A two-way ANOVA shows that in most cases, strong or weak feature is not a significant factor, therefore perceived motion directions are indistinguishable for the two feature conditions. However, when feature condition is a significant factor, such as in the case of 3:1 aperture for S1, perceived motion directions are closer to the BPI direction in the weak feature condition than in the strong feature condition ($p = 0.035$).

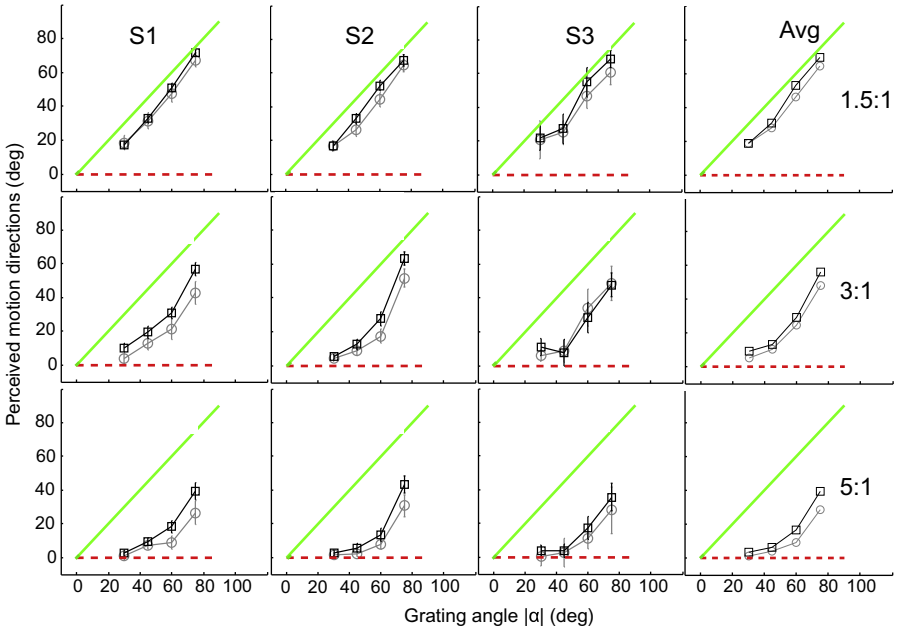

Fig. 6. Experiment 2: mean perceived motion direction (PMD) as a function of the direction $|\alpha|$ of grating motion for strong and weak feature conditions viewed in three different apertures by each of three participants. Ordinates: Mean PMDs. Abscissas: Angle $|\alpha|$ of the moving grating relative to the principle axis of the elliptical barber-pole aperture. Circles connected by light gray lines are weak feature conditions (21.5 Hz, 4% contrast), squares connected by black lines are strong feature conditions (2.75 Hz, 32% contrast). Rows represent the aspect ratios of the elliptical apertures; columns represent different participants, the fourth column is the average of the first three. The diagonal green line is the Fourier component direction, the horizontal dashed red line is the direction of the Barber-Pole Illusion (BPI). (For interpretation of the references to color in this figure legend, the reader is referred to the web version of this article.)

4.3. Conclusion

Experiment 2 shows that third-order motion (feature motion) is not only unnecessary for the BPI but it does not even strengthen the BPI when it is available. Global first-order motion (the Fourier direction of the stimuli) does have an important influence on the PMD in most stimuli, but the PMD is far from the Fourier direction. Thus, neither first- nor third-order motion computations can account for the observed PMD in Experiment 2. A probable resolution to this conundrum is that the PMDs observed in Experiment 2 (BPIs and otherwise) are caused by a higher-order process that utilizes local, not global first-order motion, e.g., the Motion Path Integration process proposed by Sun, Chubb, and Sperling (2014).[3]

5. Experiment 3: the perceived motion of reversed-phi barber-pole stimuli

Experiment 2 showed that stimulating only the first-order motion system was sufficient to produce the BPI in weak-feature stimuli; that the BPI produced by the first-order motion system was similar to or even stronger than that produced by the third-order motion system, and therefore there was no reason to postulate a third-order (feature) motion process in the BPI. Experiment 3 introduces a stimulus in which the third-order motion system (features) and the higher-order first-order motion process postulated in Experiment 2 signal motion in opposite directions. Can the first-order system generate a BPI percept even when 2D features move in a completely different direction? Can third-order feature motion produce a BPI in the presence of contradictory first-order motion? Experiment 3 addresses these questions using a novel barber-pole stimulus.

Experiment 3 was inspired by the well-known reversed-phi motion phenomenon originally described by Reichardt (1961), named by Anstis (1970), and subsequently analyzed by Chubb and Sperling (1989) and by Lu and Sperling (1999). Consider the 90°-stepping, contrast-reversing, square-wave gratings depicted in Fig. 7a. The same stimulus can appear to move upward or downward depending on which motion system dominates (Chubb & Sperling, 1989). When the stimulus is observed under conditions favoring feature-tracking (low temporal frequency, central viewing), "upward motion" is perceived because the thin bars are interpreted as features (figure versus background) and their motion is computed by the third-order motion system. When the stimulus is observed in conditions favoring the first-order system (high temporal frequency, peripheral viewing), then "downward motion" is perceived. This is because the first-order (Fourier-energy) motion is in the direction opposite to the motion direction of the narrow, contrast-reversing bars (Lu & Sperling, 1999).

5.1. Stimuli

The stimulus used in Experiment 3 was based on a contrast-reversing square-wave grating (e.g, Chubb & Sperling, 1989; Lu & Sperling, 1999) but now enclosed in an elliptical aperture (Fig. 7b). Specifically, the contrast-reversing grating was a 25% duty-cycle, 1.2 cycle/deg square-wave whose phase shifted by 90° per frame. The elliptical aperture's major and minor axes, respectively, were fixed at 4.28° and 1.07° of visual angle with hard boundaries. Throughout, grating contrast was fixed at 15%, and the stimulus contained only two contrast levels. That is, the

[3] Note that the MPI model with the same set of parameters chosen in Sun, Chubb, and Sperling (2014) predicts a near perfect BPI with slight bias towards the grating motion direction (perpendicular to the grating orientation). It does not predict the gradual shift from the BPI direction to the grating motion direction as α increases. The model parameters in Sun, Chubb, and Sperling (2014) were chosen to explain behaviors observed primarily in the peripheral viewing condition. It is very likely that, in foveal view, the best parameters may be different. To obtain optimal parameters for the foveal view requires more carefully designed experiments and is beyond the scope of the current study.

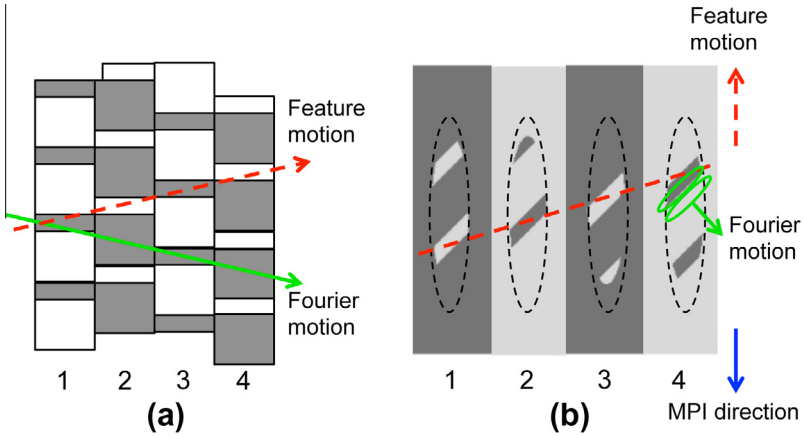

Fig. 7. The reverse-phi barber-pole stimulus of Experiment 3. (a) Space–time *y*,*t* diagram of four consecutive frames of the moving grating in the reverse-phi barber-pole stimulus. The vertical dimension *y* represents stimulus intensity along a thin vertical slice of the stimulus, the horizontal dimension represents continuous time. There are only two contrast levels in the stimulus; successive frames shift 90° and flip contrast levels. The thin rectangular bars translate to the right and up flipping contrast in successive frames; their (feature) motion is rightward-and-upward (red arrow) in the *y*,*t* diagram which represents upward motion in the stimulus. The Fourier motion-energy (white areas connect to white, black areas to black) is rightward-and-downward (green arrow) in this *y*–*t* representation, and downward and rightward in the stimulus presentation. In the spatially 2D stimulus (b), the Fourier energy is diagonally downward, something that cannot be represented in the spatially 1D representation (a). (b) Four consecutive freeze frames of a portion of the display screen that contains the reversed-phi barber-pole stimulus. The rectangular bars of the barber pole grating are visible only within the elliptical aperture denoted by the (invisible) dashed line. The entire screen (not just the area within the aperture) flips contrast on every successive frame to enhance the contrast and thereby the salience of the moving thin rectangular bars. (For interpretation of the references to color in this figure legend, the reader is referred to the web version of this article.)

background luminance was identical to that of the wider bars of the square wave gratings in each frame, and only the narrow grating bars had a different contrast. In alternate frames, the two contrast levels flipped (Fig. 7b). The image sequence was played at two temporal frequencies: 21.5 Hz (the weak-feature condition) designed to stimulate only the first-order motion system, 2.75 Hz (the strong-feature condition) designed to give a relative advantage to the third-order motion system. The relative angle of the grating was ±45°. The same three participants as in Experiments 1 and 2 participated. Subjects completed 72 trials in a mixed list in which the weak- and strong-feature stimuli were interleaved.

Of particular interest is the apparent motion of the reversed-phi barber-pole stimulus under the high temporal frequency condition. Because the feature-tracking system cannot process stimuli at such high temporal frequencies, and because the first-order system does not track features, the feature motion direction (upward in Fig. 7b) should not be reported in the weak-feature condition. Insofar as the first-order system is able to produce a BPI as in Experiment 2, the perceived motion direction should be downward, even though 2D spatial features move upward.

5.2. Results and discussion

As above, results are pooled across absolute aperture orientations, and the PMDs reported reflect angular deviations from the feature-motion direction. Data from relative angles ±45° were pooled because these two classes of stimuli are mirror symmetric with respect to feature-motion direction and do not produce statistically different results.

Fig. 8a shows the PMDs for participant S1 for both weak- and strong-feature stimuli. The data are presented as circular histograms to illustrate how tightly clustered the PMDs are. PMDs for the strong-feature (2.75 Hz) stimuli are concentrated around an angle that is very close to the feature motion direction (0°); PMDs for the weak-feature (21.5 Hz) stimuli are highly concentrated at 180°. (Note, however, that 22% (16 out of 72) of PMDs for the weak-feature stimuli are actually in the feature-motion direction.) The other two participants show very similar response patterns.

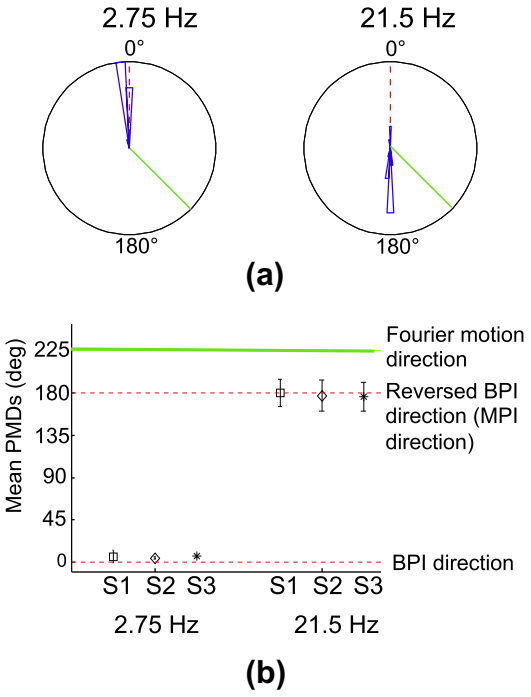

Fig. 8. Perceived motion directions (PMDs) for the reversed-phi, barber-pole stimuli used in Experiment 3. (a) Circular response histograms for participant S1, 72 trials. The entire circle is divided into 30 bins. The length of the radius of the circle corresponds to 20 occurrences. The dashed red line indicates the upward, feature motion direction. The solid green line indicates the direction corresponding to the dominant Fourier component motion direction. (b) Mean PMDs for strong-feature (left) and weak-feature (right) reversed-phi barber pole stimuli for three participants. The solid green line represents the direction of the dominant Fourier motion components. The two dashed lines represent the two opposite directions parallel to the barber-pole's orientation. Error bars represent 95% confidence interval. (For interpretation of the references to color in this figure legend, the reader is referred to the web version of this article.)

The mean PMDs for all three participants for the weak-feature (21.5 Hz) and strong-feature (2.75 Hz) stimuli are illustrated in Fig. 8b. For strong-feature stimuli, participants' PMDs are in the

feature-motion direction (along the major axis of the aperture). For weak-feature stimuli, participants' PMDs are predominantly in the direction exactly opposite the feature-motion direction (the relatively large error bars are due to the fact that participants occasionally responded to the feature-motion direction). Note in particular that the PMDs for the weak-feature stimuli are parallel to the long axis of the elliptical aperture, not in the Fourier direction perpendicular to the diagonal bars within the aperture.

5.3. Conclusion

The results of Experiment 3 confirm that two different perceptual mechanisms can produce the BPI: the first-order system can produce the BPI based on local Fourier motion-energy (and a subsequent motion-path integration process), whereas the third-order motion system can produce the BPI based on feature motion.

6. Experiment 4: the effect of a scalloped aperture boundary on the BPI

When the aperture boundary contains irregular details, the BPI is weakened (Badcock, McKendrick, & Ma-Wyatt, 2003; Kooi, 1993). Badcock, McKendrick, and Ma-Wyatt (2003) attributed the boundary effect to a system combining motion information with shape information, similar to the motion streak mechanism proposed by Geisler (1999). Experiment 4 re-examines the scalloped boundary in separate conditions in which either the first-order, energy-based or the third-order, feature-based system dominates.

6.1. Stimuli

Fig. 9a–d shows snapshots of the regularly-shaped, and the scalloped-shaped barber-pole stimuli used in Experiment 4. The regularly-shaped barber-pole was a moving sinusoidal grating (1.2 c/deg) shown in an aperture with a 3:1 aspect ratio (4.08° × 1.36°). For the irregularly-shaped barber-pole, five semicircles were present on each side of the two longer boundaries. Each semicircle had a diameter of 0.81°. The overall aspect ratio of the scalloped barber-pole was also 3:1.

The two kinds of barber-pole stimuli were shown in two conditions aiming to separate the first- and the third-order systems. In the strong-feature condition, the sinusoidal grating had a contrast of 40% and translated at 2.75 Hz. In the weak condition, the sinusoidal grating had a contrast of 4% and translated at 21.5 Hz. The barber-pole aperture boundary is inevitably less visible in the case of the low contrast, high temporal frequency grating. To improve the visibility of the irregularly-shaped aperture window, especially for the weak-feature condition, for all stimuli the background luminance (area outside of the aperture) was fixed at 46.9 cd/m^2, 10% darker than the mean luminance inside the aperture (52.1 cd/m^2).

The participants were S1, S2 and S3 (from the previous experiments) and S4 (new to the study and naive to its purposes).

6.2. Results and discussion

Fig. 10 shows the mean PMDs for the four participants and the average. In these stimuli, a perfect Barber-Pole Illusion is a PMD of 0°; the Fourier motion-energy direction is 45°. As in Experiment 2, strong and weak feature stimuli with rectangular apertures produce quite similar BPIs (Avg., 16°and 19°).

On average, in the strong-feature condition, all participants perceived a much weaker Barber-Pole Illusion for the stimuli with semicircle-edged apertures (36°) than for the stimuli with rectangular apertures (16°); the scalloped edges caused the mean PMD to deviate away from the BPI direction (0°) towards the Fourier motion energy direction by an average of 20°. In the weak feature condition, semicircle-edged apertures also produced weaker Barber-Pole Illusion (25°) compared to stimuli with rectangular apertures (19°), but the shift was only 6°.[4] Although the scalloped shape was clearly visible in both strong- and weak-feature conditions, PMDs for scalloped and plain edged apertures are much more similar in the weak- than in the strong-feature condition.

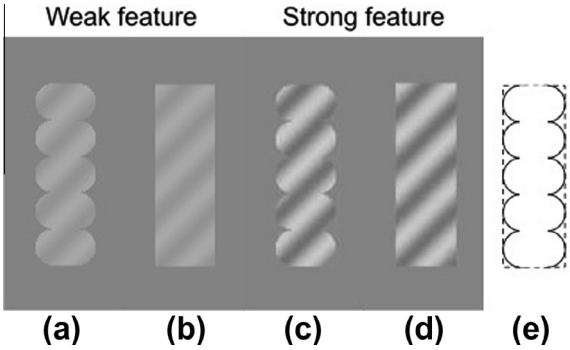

Fig. 9. Snapshots of the scalloped and classical barber pole stimuli used in Experiment 4. (a and c) The two boundaries along the aperture's major axis are composed of five semicircles (scallops). A 4% contrast sinusoidal grating moved at 21.5 Hz in (a and b) whereas a 40% contrast sinusoidal grating moved at 2.75% Hz in (c and d). (b and d) Snapshots of the regular-shaped barber-pole stimulus used in the control conditions. (e) Diagrammatic representation of a scalloped stimulus (solid lines) and a control stimulus (dashed lines). For all stimuli, the luminance of the background outside of the aperture was made 10% darker than the mean luminance inside the aperture. This served to improve the visibility of the aperture's boundary, especially when the moving grating was of low contrast and high temporal frequency. The aspect ratio of the aperture is 3:1.

The strong-feature data are consistent with the original scalloped boundary results (Kooi, 1993; Badcock, McKendrick, & Ma-Wyatt, 2003); these investigators did not study weak-feature conditions. A striking feature of the current results, consistent with the results of the other experiments reported here, is that the BPI observed for the weak-feature stimuli is as strong as or stronger than the BPI for the strong-feature stimuli in both the straight-edge and scalloped-edge conditions.

6.3. Conclusion

The influence of the aperture's scalloped boundary shape on PMD of a moving grating depends mostly on the third-order motion system's ability to resolve the features of the moving grating as they are shaped by the aperture's boundary. In weak-feature conditions in which the third-order motion system is silenced, relative to the strong-feature condition, the boundary effect is reduced from 20° to 6°, but it is still in evidence.

7. Summary and conclusion

Four experiments were conducted to determine the origin of shape–motion interactions in which the perceived motion direction (PMD) of a grating is greatly influenced by the shape of the aperture through which it is viewed. In the Barber-Pole Illusion (BPI), the PMD of a diagonally moving grating viewed through a

[4] A *t*-test reveals that, for each individual subject, the difference between the rectangular and semicircle-edged apertures is significantly greater in the strong feature condition than in the weak feature condition ($p < 0.001$). Although smaller, the deviation away from the BPI direction caused by the semicircle-edged apertures in the weak feature condition is significant for S1, S2 and S3 ($p < 0.001$). For S4, the deviation is not significant (p = 0.09).

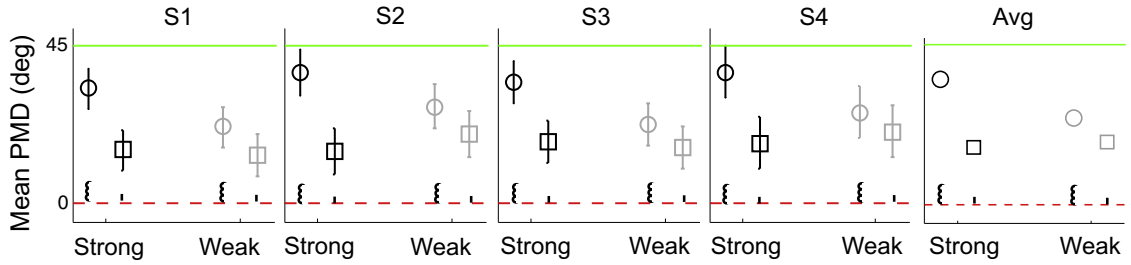

Fig. 10. Experiment 4: perceived motion direction in scalloped-edge and straight-edge barber-poles for strong- and for weak-feature gratings. Panels from left to right are for participants S1, S2, S3, S4. Circular data points are the mean PMDs for gratings in scalloped-edge barber-poles, squares represent ordinary straight-edge barber poles. Strong-feature gratings are 40% contrast, 2.75 Hz; weak-feature gratings are 4% contrast, 21.5 Hz. The continuous green line at 45° represents the direction of Fourier motion energy, the dashed red line at 0° represents the direction of the Barber-Pole Illusion (BPI). Error bars represent 95% confidence interval. (For interpretation of the references to color in this figure legend, the reader is referred to the web version of this article.)

narrow vertical aperture is aligned with the long axis of the aperture rather than with the grating's Fourier motion direction (perpendicular to the grating lines).

Experiment 1 documented the basic phenomenon, illustrating that as apertures become more elongated and as the motion direction of the moving grating more closely aligns with the major axis of the aperture, the BPI increases in strength.

Experiment 2 compared PMDs in weak-feature stimuli (21.5 Hz, 4% contrast) in which third-order (feature) motion perception was silenced, with strong-feature stimuli (2.75 Hz, 32% contrast) and found remarkably similar PMDs in both types of stimuli, i.e., stimuli accessible only to the first-order motion system produced the same BPI as classical barber-pole stimuli.

Experiment 3 compared normal with reversed-phi barber-pole stimuli in weak- and strong-feature conditions. The PMD of strong-feature stimuli was in the phi upward direction whereas the PMD of weak feature stimuli was in the opposite (Fourier, first-order motion) reverse-phi direction, demonstrating that both the first-order and the third-order motion system can each, independently, support the BPI.

Experiment 4 investigated apertures with scalloped versus smooth edges and found that the scalloped edges produced approximately a 2× greater shift of PMD direction away from BPI for strong-feature than for weak-feature stimuli.

All these results are consistent with two distinct causes of the BPI: (1) A motion-path-integration process that utilizes first-order (local Fourier) motion inputs and which operates at all temporal frequencies but is the only mechanism that can operate at very high temporal frequencies, and (2) a third-order motion process that utilizes features such as the bar-ends of the moving gratings, and which typically operates only at temporal frequencies below about 10 Hz and which, in foveal viewing of strong-feature stimuli, can dominate the first-order mechanism (Expt. 3).

Acknowledgments

This work was supported in part by NSF Award BCS-0843897. We thank the two anonymous reviewers and the editor for their helpful suggestions.

Appendix A. Fourier analysis of barber-pole displays

A barber-pole display consists of a diagonal grating $G(x,y,t)$ moving with angle α relative to the vertical that is windowed by a vertically oriented rectangle $W(x,y)$ (Fig. 1). The stimulus is defined by the product $W(x,y)G(x,y,t)$, a 3D x,y,t cube of voxels. Because the stimulus is defined by a product, the Fourier transform of the stimulus is simply the convolution of the Fourier transform

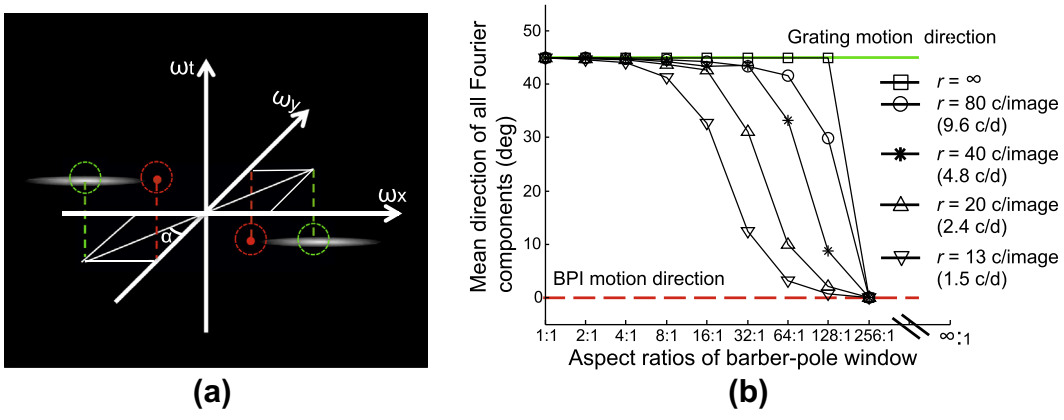

Fig. 11. Fourier analyses of classical barber-pole displays. (a) The Fourier energy spectrum of a vertically oriented barber-pole display such as one shown in Fig. 1. The center of each of the two stripes (indicated by the green circles) corresponds to the only Fourier component of a sinusoidal moving grating and to the principal component of a square grating. The convolution operation in the Fourier domain causes this grating Fourier component to be spread symmetrically by the Fourier components of the aperture window thereby producing the horizontal stripes. That is, the vertically oriented aperture window in x,y,t produces the horizontally stretched stripe in $\omega_x, \omega_y, \omega_t$. Red dots indicate where the two stripes intersect with the $\omega_y \times \omega_t$ plane, the only locations in Fourier space where Fourier energy in this stimulus would signify vertical motion. Obviously, this stimulus has essentially zero vertical motion energy, nevertheless its perceived motion direction is vertical; this is the Barber-Pole Illusion. (b) The mean direction of the visible Fourier components of a barber-pole display as a function of the aperture's aspect ratio for moving gratings. The five curves represent different spatial frequencies, r, above which stimulus spatial frequencies are assumed to be invisible: c/image refers to cycles per 256 vertical pixels, c/d refers to cycles per degree at the 60 cm experimental viewing distance. Inf is equivalent to r = 128 c/image or 15.4 c/deg. (For interpretation of the references to color in this figure legend, the reader is referred to the web version of this article.)

of W with Fourier transform of G which also is 3D with frequencies $\omega_x, \omega_y, \omega_t$. Fig. 11 illustrates the barber pole's Fourier energy spectrum in a conventional, complex-frequency representation. The BP spectrum contains two horizontal stripes centered around the Fourier component of the grating (Fig. 11a). Only components lying on the $\omega_y \times \omega_t$ plane (the red spots in Fig. 11a) signal vertical motion. As Fig. 11 shows, this typical barber-pole stimulus has essentially zero vertical motion energy. A stimulus with zero vertical motion energy that nevertheless is perceived as moving vertically constitutes an illusion, the Barber-Pole Illusion (BPI).

Are there other motion energy computations for a barber-pole stimulus that might indicate vertical motion? For example, Sperling and Liu (2009) found that for certain plaid stimuli, the first-order system computed a weighted vector summation of the visible Fourier components. Fig. 11b shows that the result of this Fourier-component-vector-summation points in the same direction as the fundamental grating component except in the most extreme, unrealistic cases. The equivalence of the direction of the vector sum of Fourier components and the direction of the fundamental Fourier component arises because the aperture spatters Fourier energy symmetrically around the fundamental grating component (where maximal energy is located).

To quantitatively describe the Fourier energy in barber pole displays, precise specifications of the barber-pole displays are required. We consider here

(1) barber-pole displays that are a sequence of 256 × 256 pixel image frames,
(2) the spatial period of the grating is 25 pixels,
(3) the relative angle α of the grating is 45°,
(4) the height of the rectangular aperture is 256 pixels,
(5) aperture widths range from 1 to 256 pixels.

The grating spatial frequency of approximately 10 cycles per image (c/image). is similar to that used in the main experiments. The mean Fourier direction, is the vector sum of all the Fourier components, each component weighted according to its energy. The results of these computations are shown in Fig. 11b.

In a 1-pixel wide vertical aperture, there is no grating, merely a point. Therefore, the Fourier motion as well as the perceived motion are vertically upward. This occurs because in the space–time domain the grating is multiplied by an impulse function, which means that in Fourier domain, the grating point is evenly distributed on a thin line extending to $\pm\infty$. Once the width of the barber pole aperture is just 2 pixels (or more), the direction of the sum of the Fourier components is indistinguishable from the (unwindowed) grating motion direction (the top curve in Fig. 11b).

Can blur produce a Fourier BPI? Suppose the highest spatial frequencies in a barber-pole display are not visible, i.e., the image is blurred. With sufficient blur, the grating segments would look like blobs, their orientation could not be detected or, at least, not well-detected. In that case, the barber-pole motion of the blobs might be perceived much like the point motion of the one-pixel-wide barber pole. Blurring cannot produce new Fourier components but, in principle, it can eliminate components not in the BPI direction and thereby unmask weak, otherwise unobservable, components in the BPI direction.

To illustrate the effect of blur, components with spatial frequencies higher than a cut-off frequency r were excluded. Different curves in Fig. 11b correspond to mean directions produced by using different values of r. Values of r are specified in c/image. Corresponding values of r in c/deg are also given based on the same viewing distance as in the main experiments (60 cm). The least amount of blur illustrated in Fig. 11b is $r = 80$ c/image corresponding to 9.6 c/deg. Normal acuity exceeds 30 c/deg; motion acuity at optimal temporal frequencies is comparable; so it is obvious that at the experimental viewing distance, even a two-pixel-wide aperture should have enough Fourier energy to destroy the BPI, which nevertheless is very strong (informal observations). What the blur computations show is that for extremely thin barber poles, at some very large viewing distance in which the stimulus details exceeds the acuity of the third-order motion system and also that of the first-order motion-path-integration mechanism, there may be a barely visible barber-pole stimulus in which the BPI occurs because of residual low-frequency Fourier motion components. In all practical cases, the visible Fourier energy in a barber-pole stimulus points in the diagonal direction of the moving grating, away from the BPI.

References

Adelson, E. H., & Bergen, J. R. (1985). Spatiotemporal energy models for the perception of motion. *Journal of the Optical Society of America A, 2*, 284–299.
Anstis, S. (1970). Phi movement as a subtraction process. *Vision Research, 10*. 1411–IN5.
Badcock, D. R., McKendrick, A. M., & Ma-Wyatt, A. (2003). Pattern cues disambiguate perceived direction in simple moving stimuli. *Vision Research, 43*, 2291–2301.
Beutter, B. R., Mulligan, J. B., & Stone, L. S. (1996). The barberplaid illusion: Plaid motion is biased by elongated apertures. *Vision Research, 36*, 3061–3075.
Brainard, D. H. (1997). The psychophysics toolbox. *Spatial Vision, 10*, 433–436.
Castet, E., Charton, V., & Dufour, A. (1999). The extrinsic/intrinsic classification of two-dimensional motion signals with barber-pole stimuli. *Vision Research, 39*, 915–932.
Castet, E., & Wuerger, S. (1997). Perception of moving lines: Interactions between local perpendicular signals and 2d motion signals. *Vision Research, 37*, 705–720.
Chubb, C., & Sperling, G. (1988). Drift-balanced random stimuli: A general basis for studying non-fourier motion perception. *Journal of the Optical Society of America A: Optics and Image Science, 5*, 1986–2007.
Chubb, C., & Sperling, G. (1989). Two motion perception mechanisms revealed through distance-driven reversal of apparent motion. *Proceedings of the National Academy of Sciences, 86*, 2985–2989.
Emerson, R. C., Bergen, J. R., & Adelson, E. H. (1992). Directionally selective complex cells and the computation of motion energy in cat visual cortex. *Vision Research, 32*, 203–218.
Fisher, N., & Zanker, J. M. (2001). The directional tuning of the barber-pole illusion. *Perception-London, 30*, 1321–1336.
Geisler, W. S. (1999). Motion streaks provide a spatial code for motion direction. *Nature, 400*, 65–68.
Kooi, F. L. (1993). Local direction of edge motion causes and abolishes the barberpole illusion. *Vision Research, 33*, 2347–2351.
Lidén, L., & Mingolla, E. (1998). Monocular occlusion cues alter the influence of terminator motion in the barber pole phenomenon. *Vision Research, 38*, 3883–3898.
Lorenceau, J. (2010). From moving contours to object motion: Functional networks for visual form/motion processing. In *Dynamics of visual motion processing* (pp. 3–36). Springer.
Lorenceau, J., & Shiffrar, M. (1992). The influence of terminators on motion integration across space. *Vision Research, 32*, 263–273.
Lorenceau, J., Shiffrar, M., Wells, N., & Castet, E. (1993). Different motion sensitive units are involved in recovering the direction of moving lines. *Vision Research, 33*, 1207–1217.
Lu, Z.-L., & Sperling, G. (1995a). Attention-generated apparent motion. *Nature, 377*, 237–239.
Lu, Z.-L., & Sperling, G. (1995b). The functional architecture of human visual motion perception. *Vision Research, 35*, 2697–2722.
Lu, Z.-L., & Sperling, G. (1999). Second-order reversed phi. *Perception & Psychophysics, 61*, 1075–1088.
Lu, Z.-L., & Sperling, G. (2001). Three-systems theory of human visual motion perception: Review and update. *Journal of the Optical Society of America A, 18*, 2331–2370.
Marshall, J. A. (1990). Self-organizing neural networks for perception of visual motion. *Neural Networks, 3*, 45–74.
Masson, G. S., Rybarczyk, Y., Castet, E., & Mestre, D. R. (2000). Temporal dynamics of motion integration for the initiation of tracking eye movements at ultra-short latencies. *Visual Neuroscience, 17*, 753–767.
Pack, C. C., Livingstone, M. S., Duffy, K. R., & Born, R. T. (2003). End-stopping and the aperture problem: Two-dimensional motion signals in macaque v1. *Neuron, 39*, 671–680.
Reichardt, W. (1961). Autocorrelation, a principle for the evaluation of sensory information by the central nervous system. *Sensory Communication*, 303–317.
Rubin, N., & Hochstein, S. (1993). Isolating the effect of one-dimensional motion signals on the perceived direction of moving two-dimensional objects. *Vision Research, 33*, 1385–1396.

Shimojo, S., Silverman, G. H., & Nakayama, K. (1989). Occlusion and the solution to the aperture problem for motion. *Vision Research, 29*, 619–626.
Sperling, G., & Liu, D. (2009). The vector sum of motion strengths describes the perceived motion direction of first-order plaids [Abstract]. *Perception, 38*, 57.
Sun, P., Chubb, C., & Sperling, G. (2014). A moving barber pole illusion. *Journal of Vision, 14*, 1–27.
Van Santen, J. P., & Sperling, G. (1984). Temporal covariance model of human motion perception. *Journal of the Optical Society of America A, 1*, 451–473.
Van Santen, J. P., & Sperling, G. (1985). Elaborated reichardt detectors. *Journal of the Optical Society of America A, 2*, 300–320.
Wallach, H. (1935). Über visuell wahrgenommene bewegungsrichtung (English translation: Wuerger, s., Shapley, R., and Rubin, N. (1996). On the visually perceived direction of motion by hans wallach: 60 years later. Perception, 25, 1317–1368). *Psychologische Forschung, 20*, 325–380.
Watson, A. B., & Ahumada, A. J. (1985). Model of human visual-motion sensing. *Journal of the Optical Society of America A, 2*, 322–342.
Weiss, Y., Simoncelli, E. P., & Adelson, E. H. (2002). Motion illusions as optimal percepts. *Nature Neuroscience, 5*, 598–604.
Yo, C., & Wilson, H. (1992). Perceived direction of moving two-dimensional patterns depends on duration, contrast and eccentricity. *Vision Research, 32*, 135–147.